Contribution from the Department of Chemistry, Faculty of Education, Mie University, Tsu, Mie 514, Japan, and Department of Chemical and Analytical Sciences, Deakin University, Geelong, Victoria 3217, Australia

Electrochemistry of Symmetrical and Asymmetrical Dinuclear Ruthenium, Osmium, and Mixed-Metal 2,2'-Bipyridine Complexes Bridged by 2,2'-Bibenzimidazolate

Masa-aki Haga*[1a] and Alan M. Bond*[1b]

Received January 17, 1990

Electrochemical studies in *n*-butyronitrile (propyl cyanide) at platinum and glassy-carbon electrodes over the temperature range −70 to +25 °C on a series of 2,2'-bibenzimidazolate- (BiBzIm-) bridged complexes of the kind $[(R^1{}_2bpy)_2M^1(BiBzIm)M^2(R^2{}_2bpy)_2](ClO_4)_2$ (M^1 and M^2 = Ru and/or Os; $R^1{}_2bpy$ and $R^2{}_2bpy$ = bypyridine ligand) reveal the presence of an extensive series of reversible one-electron-oxidation and -reduction charge-transfer processes. The combined use of mixed-metal and symmetric and asymmetric 2,2'-bipyridine ligands enables considerable information to be obtained concerning the nature of the electron-transfer processes. The reversible half-wave potentials of the oxidation processes are dependent on the metal and involve generation of oxidation state (II-III), (III-III), and (III-IV) dinuclear complexes. The potential differences in the first two oxidation processes correlate with the intervalence transfer energies. The third oxidation process leads to the formation of a reactive (III-IV) complex from which the (III-III) complex is regenerated by reaction with the solvent, light, or impurity. The predicted fourth one-electron process leading to the formation of the fully oxidized (IV-IV) dinuclear complex is not observed and is believed to be outside the available potential range in the *n*-butyronitrile solvent. The one-electron-reduction charge-transfer processes, which vary in number from four to six, are essentially 2,2'-bipyridine ligand based. Substantial changes in the potentials, observed in changing from symmetrical to asymmetrical complexes but with a relative independence on the metal, readily enable the ligand-based nature of the reduction processes to be identified in a systematic manner. The potentials for the reduction processes are discussed in terms of the π^* orbital energy levels of the 2,2'-bipyridine ligands and the strength of ligand-ligand, metal-mediated ligand-ligand, or bridging-ligand-mediated ligand-ligand interactions arising from increased electron repulsion terms associated with the reduction process.

Introduction

Electrochemical studies of complexes containing more than one redox-active metal center are inherently interesting because of the wide range of metal-metal and metal-bridging-ligand interactions. Dinuclear ruthenium and osmium complexes, which contain the metals of interest in the present study, have recently been examined with regard to metal-metal interaction in mixed-valence states[2] of the intramolecular electron- or energy-transfer process.[3] Recently, preparation and properties of some bibenzimidazolate-bridged (BiBzIm) ruthenium and osmium complexes were reported,[4] and it was noted that the complexes can be oxidized. In this paper, an extended series of complexes of the kind summarized in structure I have been prepared and both the oxidative and reductive electrochemistries of 2,2'-bibenzimidazolate-bridged ruthenium and osmium complexes and a mixed ruthenium-osmium complex are presented in detail. The complexes also contain electroactive nonbridging 2,2'-bipyridine

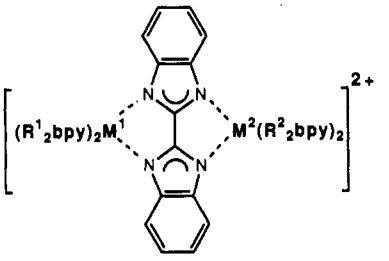

M^1	M^2	R^1	R^2
Ru	Ru	H	H
Ru	Ru	H	Me
Ru	Ru	Me	Me
Ru	Ru	H	COOEt
Ru	Os	H	H
Os	Os	H	H

I

(bpy) ligands. Although, the electrochemistries of mononuclear $[Ru(bpy)_3]^{2+}$ and its analogues have been extensively studied,[5] the corresponding electrochemical studies of dinuclear ruthenium and osmium bis(2,2'-bipyridine) complexes are relatively sparse.[6] The present extensive studies therefore provide detailed information on both metal-based pathways relevant to a dinuclear complex and organic-based electron-transfer pathways and the relative influences of the various interactions on the extensive series of electron-transfer pathways necessarily associated with complexes containing both metal and ligand redox-active centers.

Experimental Section

(a) Materials. The 2,2'-bibenzimidazolate-bridged complexes $[(bpy)_2M^1(BiBzIm)M^2(bpy)_2](ClO_4)_2$ (M^1, M^2 = Ru and/or Os), were synthesized as reported elsewhere.[4] Tetrabutylammonium perchlorate

(1) (a) Mie University. (b) Deakin University.
(2) (a) Creutz, C. *Prog. Inorg. Chem.* **1983**, *30*, 1. (b) Richardson, D. E.; Taube, H. *Coord. Chem. Rev.* **1984**, *60*, 107. (c) Meyer, T. J. *Acc. Chem. Res.* **1978**, *11*, 94. (d) Ernst, S.; Hanel, P.; Jordanov, J.; Kaim, W.; Kasack, V.; Roth, E. *J. Am. Chem. Soc.* **1989**, *111*, 1733. (e) Palaniappan, V.; Sathaiah, S.; Bist, H. D.; Agarwala, U. C. *J. Am. Chem. Soc.* **1988**, *110*, 6403. (f) Lay, P. A.; Magnuson, R. H.; Taube, H. *Inorg. Chem.* **1988**, *27*, 2364. (g) Goldsby, K. A.; Meyer, T. J. *Inorg. Chem.* **1984**, *23*, 3002. (h) Katz, N. E.; Creutz, C.; Sutin, N. *Inorg. Chem.* **1988**, *27*, 1687. (i) Kober, E. M.; Goldsby, K. A.; Narayana, D. N. S.; Meyer, T. J. *J. Am. Chem. Soc.* **1983**, *105*, 4303. (j) Bignozzi, C. A.; Roffia, S.; Scandola, F. *J. Am. Chem. Soc.* **1985**, *107*, 1644. (k) Hage, R.; Dijkhuis, A. H. J.; Haasnoot, J. G.; Prins, R.; Reedijk, J.; Buchanan, B. E.; Vos, J. G. *Inorg. Chem.* **1988**, *27*, 2185. (l) Hupp, J. T. *J. Am. Chem. Soc.* **1990**, *112*, 1563. (m) Powers, M. J.; Meyer, T. J. *J. Am. Chem. Soc.* **1980**, *102*, 1289.
(3) (a) Schmehl, R. H.; Auerbach, R. A.; Wacholtz, W. F.; Elliott, C. M.; Freitag, R. A.; Merkert, J. W. *Inorg. Chem.* **1986**, *25*, 2440. (b) Schmehl, R. H.; Auerbach, R. A.; Wacholtz, W. F. *J. Phys. Chem.* **1988**, *92*, 6202. (c) Bignozzi, C. A.; Indelli, M. T.; Scandola, F. *J. Am. Chem. Soc.* **1989**, *111*, 5192. (d) Murphy, W. R., Jr.; Brewer, K. J.; Gettliffe, G.; Petersen, J. D. *Inorg. Chem.* **1989**, *28*, 81. (e) Curtis, J. C.; Bernstein, J. S.; Meyer, T. J. *Inorg. Chem.* **1985**, *24*, 385. (f) Schanze, K. S.; Neyhart, G. A.; Meyer, T. J. *J. Phys. Chem.* **1986**, *90*, 2182. (g) Meyer, T. J. *Acc. Chem. Res.* **1989**, *22*, 163. (h) Lehn, J.-M. In *Supramolecular Photochemistry*; Balzani, V., Ed., Reidel: Dordrecht, The Netherlands, 1987; p 29. (i) Petersen, J. D. In ref 3h, p 135. (j) Shaw, J. R.; Webb, R. T.; Schmehl, R. H. *J. Am. Chem. Soc.* **1990**, *112*, 1117. (k) Bignozzi, C. A.; Roffia, S.; Chiorboli, C.; Davila, J.; Indelli, M. T.; Scandola, F. *Inorg. Chem.* **1989**, *28*, 4350.
(4) Haga, M.; Matsumura-Inoue, T.; Yamabe, S. *Inorg. Chem.* **1987**, *26*, 4148.
(5) (a) Kalyanasundaram, K. *Coord. Chem. Rev.* **1982**, *46*, 159. (b) Juris, A.; Balzani, V.; Barigelletti, F.; Campagna, S.; Belser, P. von Zelewsky, A. *Coord. Chem. Rev.* **1988**, *84*, 85. (c) Ohsawa, Y.; Hanck, K. W.; De Armond, M. K. *J. Electroanal. Chem. Interfacial Electrochem.* **1984**, *175*, 229. (d) Ghosh, B. K.; Chakravorty, A. *Coord. Chem. Rev.* **1989**, *95*, 239. (e) Kober, E. M.; Caspar, J. V.; Sullivan, B. P.; Meyer, T. J. *Inorg. Chem.* **1988**, *27*, 4587. (f) Ross, H. B.; Boldaji, M.; Rillema, D. P.; Blanton, C. B.; White, R. P. *Inorg. Chem.* **1989**, *28*, 1013. (g) Lever, A. B. P. *Inorg. Chem.* **1990**, *29*, 1271. (h) Haga, M.; Matsumura-Inoue, T.; Shimizu, K.; Sato, G. P. *J. Chem. Soc., Dalton Trans.* **1989**, 371.
(6) (a) Rillema, D. P.; Callahan, R. W.; Mack, K. B. *Inorg. Chem.* **1982**, *21*, 2589. (b) Rillema, D. P.; Mack, K. B. *Inorg. Chem.* **1982**, *21*, 3849. (c) Ernst, S. D.; Kaim, W. *Inorg. Chem.* **1989**, *28*, 1520. (d) Gex, J.-N.; Brewer, W.; Bergmann, K.; Tait, C. D.; DeArmond, M. K.; Hanck, K. W.; Wertz, D. W. *J. Phys. Chem.* **1987**, *91*, 4776. (d) Fuchs, Y.; Lofters, S.; Dieter, T.; Shi, W.; Morgan, R.; Strekas, T. C.; Gafney, H. D.; Baker, A. D. *J. Am. Chem. Soc.* **1987**, *109*, 2691. (f) Ernst, S.; Kasack, V.; Kaim, W. *Inorg. Chem.* **1988**, *27*, 1146. (g) Barigelletti, F.; De Cola, L.; Balzani, V.; Hage, R.; Haasnoot, J. G.; Reedijk, J.; Vos, J. G. *Inorg. Chem.* **1989**, *28*, 4344.

0020-1669/91/1330-0475$02.50/0

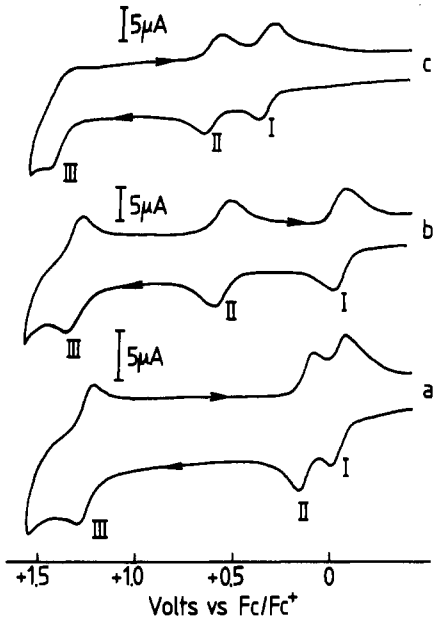

Figure 1. Cyclic voltammograms (scan rate 100 mV s^{-1}) at a glassy-carbon electrode for oxidation of $[(bpy)_2M^1(BiBzIm)M^2(bpy)_2](ClO_4)_2$ (4.7×10^{-4} mol dm^{-3}) in PrCN (0.1 mol dm^{-3} TBAP) at −73 °C: (a) $M^1 = M^2 = Os$; (b) $M^1 = Os$ and $M^2 = Ru$; (c) $M^1 = M^2 = Ru$.

(TBAP) was synthesized by metathesis of tetrabutylammonium bromide (Tokyo Kasei) and sodium perchlorate in water, recrystallized from ethanol three times, and vacuum-dried at 70 °C for at least 5 h. $Ru(R_2bpy)_2Cl_2$ (R = H, Me, COOEt) complexes were prepared by literature methods.[7] Acetonitrile and *n*-butyronitrile, which is also known as propyl cyanide (PrCN) were initially dried over phosphorus pentoxide and then over calcium hydride before use.

(b) Preparation of New Complexes. $[(bpy)_2Ru(BiBzIm)Ru(R_2bpy)_2](ClO_4)_2$ (R = Me or COOEt). *cis*-$Ru(Me_2bpy)_2Cl_2$ (0.3 g, 0.55 mmol) was suspended in ethanol/water (1:1 v/v, 50 cm^3) and heated for 1 h under nitrogen. An equivalent amount of $Ru(bpy)_2(BiBzIm)\cdot 2H_2O$ (0.37 g, 0.55 mmol) was added, and the mixture was further refluxed for 5 h. The resulting solution was cooled to room temperature and filtered. A methanol solution of sodium perchlorate (0.46 g, 3.3 mmol) was added to the filtrate. The brown precipitate was isolated by filtration and recrystallized from acetonitrile/ether; 36% yield. The complex with R = COOEt was similarly obtained except that *cis*-$Ru(EtCOO_2bpy)_2Cl_2$ was used to give a 42% yield. Anal. Calcd for $C_{58}N_{48}N_{12}Cl_2O_8Ru_2\cdot 4H_2O$ (R = Me): C, 50.25; H, 2.65; N, 12.12. Found: C, 50.08; H, 3.56; N, 11.88. Calcd for $C_{66}H_{56}N_{12}O_8Cl_2Ru_2\cdot 10H_2O$ (R = COOEt): C, 49.59, H, 4.79; N, 10.51. Found: C, 49.04; H, 3.51; N, 10.34.

$[(Me_2bpy)_2Ru(BiBzIm)Ru(Me_2bpy)_2](ClO_4)_2$. $[Ru(Me_2bpy)_2(BiBzImH_2)](ClO_4)_2$ (0.3 g, 0.33 mmol) was dissolved in methanol (40 cm^3) by heating. To the resulting solution was added sodium metal (0.04 g, 1.8 mmol). The initially dark red solution immediately became violet in color. Solid $Ru(Me_2bpy)_2Cl_2$ (0.18 g, 0.33 mmol) was added, and the mixture was further heated under reflux for 6 h. The solution was cooled to room temperature and then filtered. An excess of sodium perchlorate (0.3 g, 2.3 mmol) in methanol (10 cm^3) was added to the filtrate. The dark brown microcrystalline precipitate was isolated by filtration and recrystallized from acetonitrile/ether; 35% yield. Anal. Calcd for $C_{62}H_{56}N_{12}O_8Cl_2Ru_2\cdot 4H_2O$: C, 51.63; H, 4.47; N, 11.65. Found: C, 51.64, H, 4.37; N, 11.36.

(c) Physical Measurements. Electrochemical measurements were made at 25 °C with a Bioanalytical Systems BAS-100 electrochemical analyzer, a Princeton Applied Research (PAR) Model 174 polarographic analyzer with a Houston Model 2000 X-Y recorder, or a Yanagimoto P-1100 voltammetric analyzer with a Watanabe WX-4401 X-Y recorder. The working electrodes were glassy-carbon or platinum disks and the auxiliary electrode was a platinum wire or platinum plate. The reference electrode, separated from the cell by a salt bridge, was Ag/AgCl (acetone, saturated with dry LiCl) or $Ag/AgNO_3$ (0.01 mol dm^{-3} in CH_3CN). The ferrocene–ferrocenium (Fc/Fc^+) redox couple was measured via voltammetric oxidation of a 5×10^{-4} mol dm^{-3} solution of ferrocene to provide an internal reference, and all potentials were referred to those for the Fc/Fc^+ couple.[8] A Metrohm rotating disk electrode assembly, Model 628-10, was used for the hydrodynamic voltammetry. Coulometry was undertaken by using a PAR Model 173 potentiostat and a PAR Model 179 digital coulometer at a platinum-gauze working electrode. The reference electrode was the same Ag/AgCl electrode used in the voltammetric experiments, and the auxiliary electrode was platinum gauze separated from the test solution by a salt bridge containing the solvent mixture.

Electronic spectra were recorded on a Hitachi U-3200 (250–850-nm region) or 3400 (900–2500-nm region) spectrophotometer. The spectroelectrochemistry was performed by using a platinum-minigrid (80 mesh) working electrode in a cell designed originally by Lexa et al.[9]

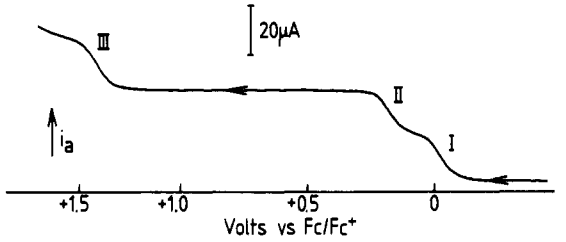

Figure 2. Rotating disk voltammogram for the oxidation of $[(bpy)_2Os(BiBzIm)Os(bpy)_2](ClO_4)_2$ in PrCN (0.1 mol/dm^{-3} TBAP) at 20 °C at a glassy-carbon electrode. Scan rate = 20 mV s^{-1}, and rotation rate of electrode = 1000 rpm.

Results and Discussion

Oxidation Processes of BiBzIm-Bridged Dinuclear Complexes. A limited set of results have been reported for some of the complexes over a narrow potential range.[4] The wide potential range available in the present study with an extended series of complexes provides a far more comprehensive data set.

Figure 1a shows a cyclic voltammogram for oxidation of the osmium dinuclear complex $[(bpy)_2Os(BiBzIm)Os(bpy)_2](ClO_4)_2$ in PrCN (0.1 mol dm^{-3} TBAP) at a glassy-carbon electrode at −73 °C. Three well-defined oxidation processes labeled I, II, and III respectively are observed. Processes I and II are chemically reversible at both room temperature and low temperature. However, process III is chemically irreversible at room temperature. The use of low temperatures (−73 °C) and fast scan rates causes process III to become reversible as the influence of a chemical reaction following the third oxidation charge-transfer process is eliminated. Bulk controlled-potential electrolysis experiments on $[(bpy)_2Os(BiBzIm)Os(bpy)_2](ClO_4)_2$ at potentials slightly more positive than their peak potentials for process I or II at 20 °C confirmed that these are both one-electron-oxidation processes (coulometry). In contrast, bulk electrolysis at potentials corresponding to process III with coulometric monitoring gives an *n* value for the number of electrons transferred as being 1.8 ± 0.2 at 20 °C. Rotating disk voltammograms obtained after electrochemical oxidation of the solution demonstrates that an (80 ± 5)% regeneration of Os(III)–Os(III) complex has occurred. This regeneration process is accompanied by a (20 ± 5)% decomposition reaction. The bulk electrolysis data demonstrate that on long time scale experiments that process III includes a catalytic step in which Os(III)–Os(III) is regenerated, by reaction with solvent, light, or an impurity or via other processes.

The rotating disk voltamogram of $[(bpy)_2Os(BiBzIm)Os(bpy)_2](ClO_4)_2$ at a glassy-carbon electrode in PrCN is shown in Figure 2. Voltammograms before and after electrolysis for process I or II were the same except for the expected change in the current sign, thereby confirming the chemical reversibility of these processes. The limiting current of process III at a rotating disk electrode is the same as that of process I or II, which means that the process III corresponds to a one-electron-oxidation process

(7) (a) Sprintschnik, G.; Sprintschnik, H. W.; Kirsch, P. P.; Whitten, D. G. J. *J. Am. Chem. Soc.* **1977**, *99*, 4947. (b) Elliott, C. M.; Hershenhart, E. J. *J. Am. Chem. Soc.* **1982**, *104*, 7519.

(8) Gagne, R. R.; Koval, C. A.; Lisensky, G. C. *Inorg. Chem.* **1980**, *19*, 2854.

(9) Lexa, D.; Saveant, J. M.; Zickler, J. *J. Am. Chem. Soc.* **1977**, *99*, 2786.

Table I. Electrochemical Data for Oxidation and Reduction of $[(R^1{}_2bpy)_2M^1(BiBzIm)M^2(R^2{}_2bpy)_2](ClO_4)_2$ in PrCN at a Glassy-Carbon Electrode at 20 °C

				$E_{1/2}$,[a] V vs Fc/Fc^+							
				oxidation			reduction				
M^1	M^2	R^1	R^2								
Ru	Ru	H	H	+1.414	+0.640	+0.348	−1.914 (2)[b]	−2.234	−2.314		
Ru	Ru	H	Me	+1.412	+0.633	+0.306	−1.899	−2.019	−2.230	−2.367	
Ru	Ru	Me	Me	+1.419	+0.542	+0.249	−2.033 (2)[b]	−2.315	−2.422		
Ru	Ru	H	COOEt		+0.807	+0.419	−1.451	−1.704	−1.938	−2.233 (2)	−2.511
Ru	Os	H	H	+1.356	+0.592	−0.020	−1.894 (2)[b]	−2.218	−2.294		
Os	Os	H	H	+1.296	+0.152	−0.036	−1.878 (2)[b]	−2.254	−2.318		

[a] Data obtained from differential pulse voltammetry. [b] The numbers of electrons involved in the unresolved charge-transfer processes are given in parentheses.

on the voltammetric time scale. Thus, the electrode process can be written as follows:

$$[(bpy)_2Os(BiBzIm)Os(bpy)_2]^{2+} \rightleftharpoons [(bpy)_2Os(BiBzIm)Os(bpy)_2]^{3+} + e^- \quad (1)$$

$$[(bpy)_2Os(BiBzIm)Os(bpy)_2]^{3+} \rightleftharpoons [(bpy)_2Os(BiBzIm)Os(bpy)_2]^{4+} + e^- \quad (2)$$

$$[(bpy)_2Os(BiBzIm)Os(bpy)_2]^{4+} \rightleftharpoons [(bpy)_2Os(BiBzIm)Os(bpy)_2]^{5+} + e^- \quad (3)$$

$$[(bpy)_2Os(BiBzIm)Os(bpy)_2]^{4+} \xrightarrow{\text{slow}} \text{product(s)}$$

The cyclic voltammograms of $[(bpy)_2M^1(BiBzIm)M^2(bpy)_2]^{2+}$ (M^1, M^2 = Ru or M^1 = Ru, M^2 = Os) in PrCN (0.1 mol dm^{-3} TBAP) are shown in Figure 1b,c. As is the case with the osmium dinuclear complex, three oxidation processes, processes I, II and III, are observed. Process III is chemically reversible for the RuOs dinuclear complex, at −73 °C and a scan rate of 100 mV s^{-1}, but is chemically irreversible for the RuRu complex under the same conditions. Processes I and II for the RuRu complex occur at much more positive potentials than those for the OsOs complex as would be expected for metal-based processes. That is, the Os complexes are easier to oxidize than their Ru analogues, which is consistent with the general redox properties of third-row vs second-row transition-metal complexes.[10] However, it is interesting to note that process I for the mixed OsRu complex occurs at a potential that is similar to process I for the OsOs complex whereas process II for the OsRu complex occurs midway between processes I and II for the RuRu complex. That is, process I for the mixed complex has thermodynamic properties consistent with oxidation of an osmium cation whereas process II has properties consistent with oxidation of a ruthenium cation. Process III occurs at a similar potential for all complexes.

The pattern of oxidative voltammetric behavior for other RuRu dinuclear complexes is almost parallel with that for the RuRu complex described above. The reversible half-wave potentials ($E^r{}_{1/2}$) for oxidation of all complexes studied are collected in Table I. The reversible potentials for oxidation processes I and II, which may be predominantly associated with M(II)/M(III) redox couples, are strongly dependent on the central metal ion M^1 and M^2 and the substituent on the bpy ligand. On the other hand, the variation of the reversible oxidation potential for process III, which may be associated with a M(III)/M(IV) process, is smaller than that for processes I and II. In previous studies of Ru and Os mononuclear complexes, the M(III)/M(IV) couple (M = Ru and Os) is reported to be less sensitive than the M(II)/M(III) couple to the change of ligands around the central metal ion.[11]

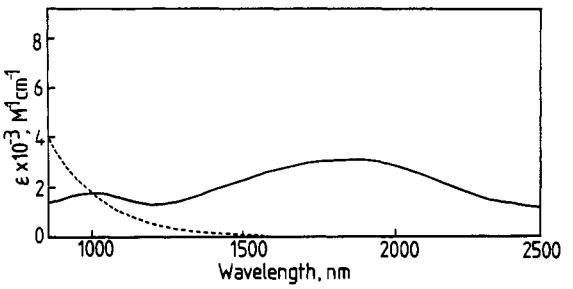

Figure 3. Near-infrared spectra of $[(bpy)_2Ru(BiBzIm)Ru(Me_2bpy)_2]^{n+}$ (2.29×10^{-3} mol dm^{-3}; optical cell length = 0.05 cm) after electrochemical oxidation in CH_3CN (0.1 mol dm^{-3} TBAP): after electrolysis at +0.4 V (n = 3, —) and at +0.9 V (n = 4, --) vs Fc/Fc^+.

Apparently, a similar tendency holds for dinuclear complexes. Attempts to observe the predicted fourth oxidation process, which should correspond to a M(III-IV)/M(IV-IV) process, have failed. Presumably, the potential for the process occurs at a more positive potential than that for the solvent oxidation limit.

The potential difference between the first and second oxidation processes, $\Delta E_{1/2}$, is dependent on the temperature. For the symmetric $[(bpy)_2M^1(BiBzIm)M^2(bpy)_2]^{2+}$ complex, the $\Delta E_{1/2}$ value becomes smaller when the temperature is lowered; that is, $\Delta E_{1/2}$ = 0.292 V at 20 °C and 0.262 V at −70 °C for M^1 = M^2 = Ru, and $\Delta E_{1/2}$ = 0.188 V at 20 °C and 0.168 V at −78 °C for M^1 = M^2 = Os. The temperature coefficient of the electrode potential has been used to determine the reaction entropies for $[(Ru(bpy)_2Cl)_2(pyz)]^{2+}$; the reaction entropies for the separate redox steps, $\Delta S_1°$ and $\Delta S_2°$, are the same, which indicates that the identically coordinated Ru ions act as if they are two structurally independent redox centers.[12] In the present case, the reaction entropy $\Delta S°$ (= $\Delta S_1°$ = $\Delta S_2°$) is estimated to be about 5–6 cal deg^{-1} mol^{-1}. That is, the mixed-valence BiBzIm-bridged complexes have a small degree of communication between M(II) and M(III) ions and are not completely independent redox centers.

Correlation of the Oxidation Potential Difference and Intervalence Energies. The stability of the mixed-valence complexes can be estimated from the comproportionation constant K_{com} as follows:

$$[M^{II}\text{-BiBzIm-}M^{II}]^{2+} + [M^{III}\text{-BiBzIm-}M^{III}]^{4+} \xrightleftharpoons{K_{com}} 2[M^{II}\text{-BiBzIm-}M^{III}]^{3+} \quad \Delta E = 0.0591 \log K_{com} \text{ (at 25 °C)}$$

The present dinuclear Ru and Os complexes have relative large K_{com} values (1.5×10^3 to 3.8×10^6), which indicates the mixed-valence complexes are stable. This stability arises mainly from the electronic attraction between the anionic bridging BiBzIm ligand and metal cations and electronic delocalization through the BiBzIm bridging ligand, as discussed elsewhere.[4]

All the dinuclear complexes exhibit rich near-infrared spectra after the stepwise oxidative electrolysis. Figure 3 shows the near-infrared spectra of $[(bpy)_2Ru(BiBzIm)Ru(Me_2bpy)_2]^{n+}$ (n = 2–4). While the complex with the Ru(II)–Ru(II) oxidation

(10) (a) Pyykko, P.; Desclaux, J.-P. *Acc. Chem. Res.* **1979**, *12*, 276. (b) Heath, G. A.; Moock, K. A.; Sharp, D. W. A.; Yellowlees, L. J. *J. Chem. Soc., Chem. Commun.* **1985**, 1503. (c) Taube, H. *Pure Appl. Chem.* **1979**, *51*, 901.

(11) Bond, A. M.; Haga, M. *Inorg. Chem.* **1986**, *25*, 4507.

(12) Schmitz, J. E. J.; van der Linden, J. G. M. *Inorg. Chem.* **1984**, *23*, 117.

Table II. Intervalence Transfer Band Parameters for Mixed-Valence $[(R^1{}_2bpy)_2M^1(BiBzIm)M^2(R^2bpy)_2]^{3+}$ Complexes Generated by Oxidative Controlled-Potential Electrolysis in CH_3CN

M^1	M^2	R^1	R^2	$\lambda_{max}(1)$, nm	ϵ, dm^3 mol^{-1} cm^{-1}	$\lambda_{max}(2)$, nm	ϵ, dm^3 mol^{-1} cm^{-1}	$\Delta E_{1/2}$,[a] V
Ru	Ru	H	H	1062	1300	1950	3400	0.292
Ru	Ru	H	Me	994	1700	1855	3200	0.327
Ru	Ru	Me	Me	1011	1700	1999	4650	0.293
Ru	Ru	H	COOEt	1030	2100	1445	2160	0.388
Ru	Os	H	H	1044	1430	1792	810	0.612

[a] Potential difference between the first and second oxidation processes in PrCN.

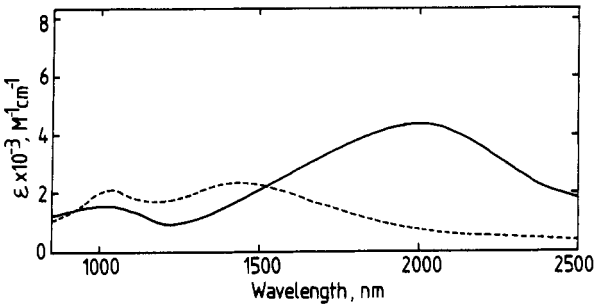

Figure 4. Near-infrared spectra of mixed-valence $[(Me_2bpy)_2Ru(BiBzIm)Ru(Me_2bpy)_2](ClO_4)_3$ (—) and $[(bpy)_2Ru(BiBzIm)Ru(EtOCO_2bpy)_2](ClO_4)_3$ (--) generated by electrochemical oxidation in CH_3CN (0.1 mol dm^{-3} TBAP).

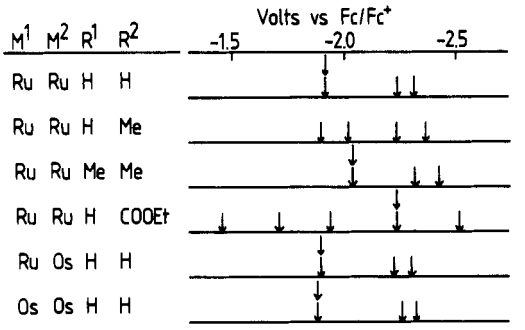

Figure 5. Reduction patterns of a series of BiBzIm-bridged dinuclear complexes in PrCN (0.1 mol dm^{-3} TBAP) at 20 °C.

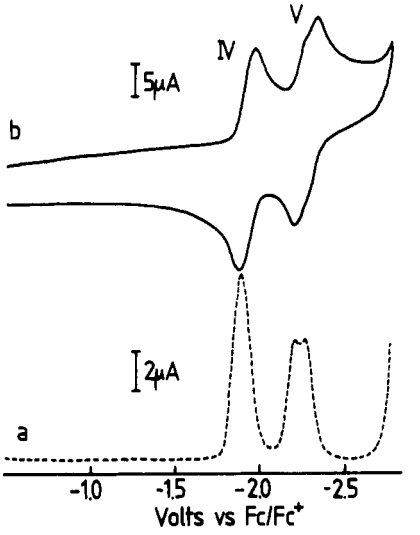

Figure 6. Differential pulse voltammogram (a) (scan rate = 4 mV s^{-1}) and a cyclic voltammogram (b) (scan rate = 100 mV s^{-1}) for the reduction of $[(bpy)_2Os(BiBzIm)Os(bpy)_2](ClO_4)_2$ in PrCN (0.1 mol dm^{-3} TBAP) at a glassy-carbon electrode at 20 °C.

state is transparent with respect to its infrared spectrum, the mixed-valence complex shows two bands at 5390 and 9710 cm^{-1}. The Ru(III)–Ru(III) complex exhibits only the tail of an absorption maximum at 744 nm, which is assigned to the ligand-to-metal charge-transfer (LMCT) transition, with the bands at 5390 and 9710 cm^{-1} associated with the mixed-valence compound being completely absent. Thus, the bands at 5390 and 9710 cm^{-1} can be assigned as intervalence charge-transfer (IT) bands. The IT bands are considered to arise from the different electronic components of the IT transition, which are attributable to the t_{2g} orbital splitting into $d\pi_1$, $d\pi_2$, and $d\pi_3$ orbitals because of spin–orbit coupling. It has already been shown that multiple IT transitions are observed for mixed-valence Os dinuclear complexes, where the spin–orbit coupling is large (~3000 cm^{-1}).[2i,13] Since the spin–orbit coupling constant of Ru is about 1100 cm^{-1}, the three components associated with the IT transition have usually been overlapped and therefore observed apparently as one band.[14] However, all the BiBzIm-bridged dinuclear Ru complexes described in this paper show similar multiple IT bands in the near-infrared region (see Figure 4). While the higher energy IT band is almost independent of the potential difference between the first and second oxidation potentials for the Ru dinuclear complexes, the lower energy IT band is shifted to the shorter wavelength when the potential difference increases. This result indicates that some features of the two IT bands are different and that more detailed studies are required to properly assign the origin of the multiple IT bands. A multiple IT band also has been reported for the $[(NH_3)_5Ru(benzoquinone\ diimine)Ru(NH_3)_5]^{5+}$ complex.[15]

The Os_2 and RuOs dinuclear complexes exhibit more complicated near-infrared spectra than that described above for the Ru_2 complex. Since the Os(III) complexes exhibit $d\pi$–$d\pi$ transitions in the 1800–2500-nm region, as expected the same $d\pi$–$d\pi$ transitions are also seen for the other Os(III) containing dinuclear complexes such as the Ru(II)–Os(III), Os(II)–Os(III), and Os(III)–Os(III) complexes. The IT bands can be observed by subtracting the $d\pi$–$d\pi$ transitions for the Os(III) component(s) from the original near-infrared spectra. The IT bands are collected in Table II, and it can be seen that multiple IT bands are also observed for the Os_2 and RuOs dinuclear complexes.

Introduction of redox asymmetry into the dinuclear complexes by making either a mixed-metal or mixed-ligand complex results in a change in the Franck–Condon energy. Recently, the relationship between the electrochemically determined redox asymmetry and the spectroscopic IT band energies has been described for a series of asymmetric $[(bpy)_2RuCl(pyz)Ru(NH_3)_4L]^{4+}$, and a 1:1 energetic relationship $\delta E_{IT}\delta(\Delta E_{1/2}) = 1$ has been reported.[16] A linear correlation between E_{IT} and $\Delta E_{1/2}$ also is obtained for the present system. However, the slopes are 1.91 (lower energy IT band) and 0.09 (higher energy IT band) for four Ru dinuclear complexes. The deviation from the predicted slope of 1 probably may be attributed to the change in the ground state of the Ru(II) and Ru(III) sites that occurs when a substituent is introduced onto the bpy ligand. That is, the stable oxidation states in mixed-valence complexes are $[(bpy)_2Ru^{II}(BiBzIm)Ru^{III}(R_2bpy)_2]^{3+}$ (R = H and EtOCO) and $[(Me_2bpy)_2Ru^{II}(BiBzIm)Ru^{III}(R_2bpy)_2]^{3+}$ (R = H and Me). If the shape of the potential energy surfaces for the ground and excited states are changed in the complexes considered in this study, the quantity $\delta E_{IT}/\delta(\Delta E_{1/2})$ can be ex-

(13) (a) Hudson, A.; Kennedy, M. J. *J. Chem. Soc. A* **1969**, 1116. (b) Kober, E. M.; Meyer, T. J. *Inorg. Chem.* **1983**, *22*, 1614.
(14) Hupp, J. T.; Meyer, T. J. *Inorg. Chem.* **1987**, *26*, 2332.
(15) Joss, S.; Burgi, H. B.; Ludi, A. *Inorg. Chem.* **1985**, *24*, 949.
(16) Chang, J. P.; Fung, E. Y.; Curtis, J. C. *Inorg. Chem.* **1986**, *25*, 4233.

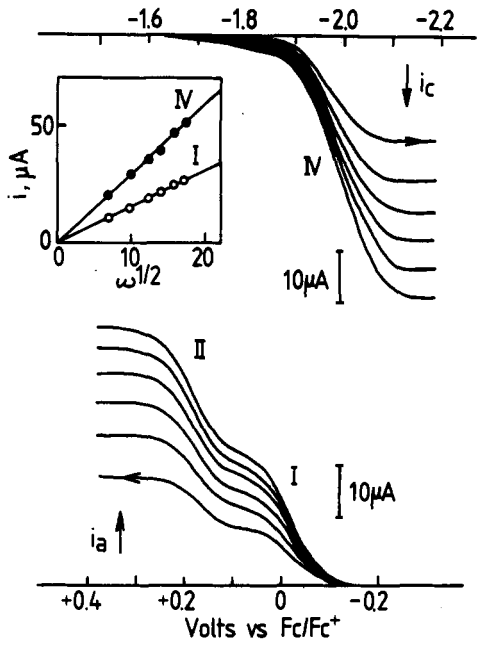

Figure 7. Rotating disk voltammograms at a glassy-carbon electrode of $[(bpy)_2Os(BiBzIm)Os(bpy)_2](ClO_4)_2$ in PrCN containing 0.1 mol dm^{-3} TBAP at 20 °C. Scan rate = 20 mV s^{-1}. The electrode rotation rates are 500, 1000, 1500, 2000, 2500, and 3000 rpm, respectively.

pected to deviate from the unity as has in fact been observed.

Reduction Processes of BiBzIm-Bridged Dinuclear Complexes. The reduction processes are characterized by a series of reversible steps whose potentials are summarized in Figure 5 and Table I.

(i) Symmetrical Dinuclear Complexes. Figure 6 shows a cyclic voltammogram and a differential-pulse voltammogram for the reduction of $[(bpy)_2Os(BiBzIm)Os(bpy)_2]^{2+}$ in PrCN at 20 °C. Two chemically reversible reduction waves, labeled as processes IV and V, are observed. However, process V is resolved into two closely spaced peaks (one-electron processes) in the differential-pulse voltammogram. A two-electron process for the first reduction wave is confirmed by comparison of the height of the diffusion-controlled limiting current with the known one-electron-oxidation processes (I or II) observed under conditions of rotating disk voltammetry (Figure 7). The peak to peak separation of process IV in cyclic voltammetry is 100 mV, which is considerably larger than the theoretically predicted value of 28 mV for a reversible two-electron-reduction process. This result may be explained if process IV actually consists of two stepwise one-electron-reduction processes with similar half-wave potentials rather than a single two-electron process. The reduction potentials for processes IV and V are almost constant even when the central Os metal is replaced by Ru in the dinuclear complex. This suggests that reduction processes IV and V are ligand-based. Since the BiBzIm ligand acts as a π donor, the π^* orbitals associated with BiBzIm are at much higher energies than those of bpy. Therefore, bpy can be regarded as the electroactive ligand. Furthermore, the monomeric complex, $[Ru(bpy)_2(BiBzImH_2)]^{2+}$, has been reported to exhibit two bpy ligand-based processes at potentials more negative than −2.0 V vs SCE.[17] Thus, it can be concluded that four one-electron-reduction processes based on the bpy ligand are observed in the dinuclear complexes.

To further elucidate the reduction site in the dinuclear complexes, the reductive spectroelectrochemistry of $[(bpy)_2Ru(BiBzIm)Ru(bpy)_2]^{2+}$ was investigated at a potential of −2.1 V vs Fc/Fc^+ in CH_3CN. However, some decomposition of the reduced complex occurred during the course of electrolysis as evidenced by observation of a decrease of the absorbance without the presence of any isosbestic points. However, new bands generated during the initial stage of the reductive electrolysis at 536 and 500 nm correspond to the $\pi\pi^*$ transition in bpy^-.[18] This result strongly supports the suggestion that the reduction processes are bpy ligand-based, but decomposition of the initially formed complex occurs on the synthetic or bulk electrolysis time scale.

The theoretical maximum number of the ligand-localized reduction processes that can be observed has been proposed to be related to the number of electrons that can be localized by ligands.[19] The existence of four substituted bpy ligands in the present symmetrical dinuclear complexes can be expected to show a maximum of eight reduction steps. However, only four reduction processes are observed within the accessible potential range. Since two $M(bpy)_2$ moieties are separated by a BiBzIm bridge, the interactions of the bpy ligand between the different moieties are relatively small. Thus, the first electrons added to the dinuclear complexes are predicted to be localized in a bpy ligand on each $M(bpy)_2$ moiety (eqs 4 and 5). Further electrons may be accepted by the other bpy ligands on each $M(bpy)_2$ moiety at a more negative potential (eqs 6 and 7). Thus, the reduction processes can be summarized by eqs 4–7. The separation of the reduction

$$[(bpy)_2Os(BiBzIm)Os(bpy)_2]^{2+} + e^- \rightleftharpoons [(bpy)(bpy^-)Os(BiBzIm)Os(bpy)_2]^+ \quad (4)$$

$$[(bpy)(bpy^-)Os(BiBzIm)Os(bpy)_2]^+ + e^- \rightleftharpoons [(bpy)(bpy^-)Os(BiBzIm)Os(bpy)(bpy^-)] \quad (5)$$

$$[(bpy)(bpy^-)Os(BiBzIm)Os(bpy)(bpy^-)] + e^- \rightleftharpoons [(bpy^-)_2Os(BiBzIm)Os(bpy)(bpy^-)]^- \quad (6)$$

$$[(bpy^-)_2Os(BiBzIm)Os(bpy)(bpy^-)]^- + e^- \rightleftharpoons [(bpy^-)_2Os(BiBzIm)Os(bpy^-)_2]^{2-} \quad (7)$$

potential between the first and second processes (eqs 4 and 5) is smaller than that between the third and fourth ones (eqs 6 and 7), which can be attributed to the electronic repulsion energy as pointed out by Vlcek.[19] Parallel behavior is observed for both the symmetrical $[(bpy)_2Ru(BiBzIm)Ru(bpy)_2]^{2+}$ and $[(Me_2bpy)_2Ru(BiBzIm)Ru(Me_2bpy)_2]^{2+}$ complexes (Table I).

(ii) Asymmetrical Dinuclear Complexes. If the concept of the reduction processes being ligand-based is correct, then asymmetrical Ru dinuclear complexes having two different substituted bpy ligand moieties (different ligand π^* orbital energies) should exhibit well-separated reduction process. Figure 8 shows a cyclic voltammogram and a differential-pulse voltammogram for the reduction of the asymmetrical $[(bpy)_2Ru(BiBzIm)Ru(EtCOO_2bpy)_2]^{2+}$ complex. Five reduction processes are observed. The potentials for the first two sequential one-electron reductions in $[(bpy)_2Ru(BiBzIm)Ru(EtCOO_2bpy)_2]^{2+}$ are shifted in the positive potential direction relative to those for the symmetrical $[(bpy)_2Ru(BiBzIm)Ru(bpy)_2]^{2+}$ complex. The third reduction process is also a one-electron process. The next reduction process consists of two unresolved one-electron processes. The final (most negative) process also is a one-electron process. The number of electrons in each process is confirmed by comparison of the height of the limiting current with the known one-electron oxidation processes. Since the π^* energy level of the $EtCOO_2bpy$ ligand is lower than that of unsubstituted bpy, the first two electrons in the reduction of $[(bpy)_2Ru(BiBzIm)Ru(EtCOO_2bpy)_2]^{2+}$ are placed into $EtCOO_2bpy$ ligands. The third reduction potential is almost the same as the first reduction potential for the symmetrical complex $[(bpy)_2Ru(BiBzIm)Ru(bpy)_2]^{2+}$. However, the increase of the negative charge should be important since the reduction of bpy ligand in $(bpy)_2Ru(BiBzIm)Ru(EtCOO_2bpy)_2$ is expected to be shifted toward more negative potentials than that for the reduction of $[(bpy)_2Ru(BiBzIm)Ru(bpy)_2]^{2+}$. Thus, the next two reduction steps can also be assumed to occur on the reduced $EtCOO_2bpy$ ligands. The last two reduction processes

(17) Haga, M. *Inorg. Chim. Acta* **1983**, *75*, 29.

(18) (a) Heath, G. A.; Yellowlees, L. J.; Braterman, P. S. *J. Chem. Soc., Chem. Commun.* **1981**, 287. (b) Coombe, V. T.; Heath, G. A.; MacKenzie, A. J.; Yellowlees, L. J. *Inorg. Chem.* **1984**, *23*, 3423.

(19) Vlcek, A. A. *Coord. Chem. Rev.* **1982**, *43*, 39.

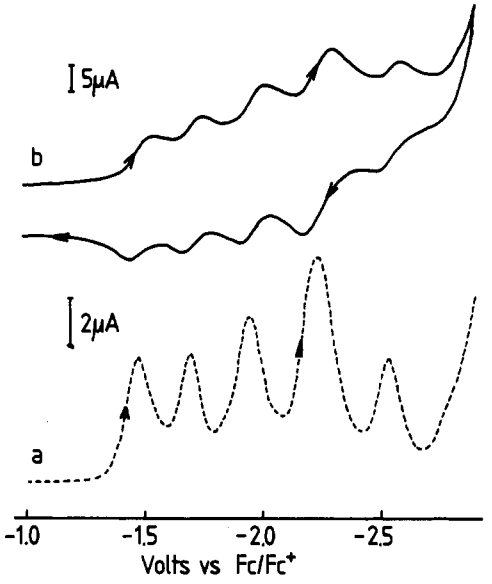

Figure 8. Differential pulse voltammogram (a) (scan rate = 4 mV s^{-1}) and a cyclic voltammogram (b) (scan rate = 100 mV s^{-1}) at a glassy-carbon electrode for the reduction of $[(bpy)_2Ru(BiBzIm)Ru(EtOCO_2bpy)_2](ClO_4)_2$ in PrCN (0.1 mol dm^{-3} TBAP) at 20 °C.

therefore are based on those of the unsubstituted bpy ligands.

The reduction processes can be summarized as follows:

$$[(bpy)_2Ru(BiBzIm)Ru(EtCOO_2bpy)_2]^{2+} + e^- \rightleftharpoons [(bpy)_2Ru(BiBzIm)Ru(EtCOO_2bpy)(EtCOO_2bpy^-)]^+ \quad (8)$$

$$[(bpy)_2Ru(BiBzIm)Ru(EtCOO_2bpy)(EtCOO_2bpy^-)]^+ + e^- \rightleftharpoons [(bpy)_2Ru(BiBzIm)Ru(EtCOO_2bpy^-)_2] \quad (9)$$

$$[(bpy)_2Ru(BiBzIm)Ru(EtCOO_2bpy^-)_2] + e^- \rightleftharpoons [(bpy)_2Ru(BiBzIm)Ru(EtCOO_2bpy^-)(EtCOO_2bpy^{2-})]^- \quad (10)$$

$$[(bpy)_2Ru(BiBzIm)Ru(EtCOO_2bpy^-)(EtCOO_2bpy^{2-})]^- + e^- \rightleftharpoons [(bpy)_2Ru(BiBzIm)Ru(EtCOO_2bpy^{2-})_2]^{2-} \quad (11)$$

$$[(bpy)_2Ru(BiBzIm)Ru(EtCOO_2bpy^{2-})_2]^{2-} + e^- \rightleftharpoons [(bpy)(bpy^-)Ru(BiBzIm)Ru(EtCOO_2bpy^{2-})_2]^{3-} \quad (12)$$

$$[(bpy)(bpy^-)Ru(BiBzIm)Ru(EtCOO_2bpy^{2-})_2]^{3-} + e^- \rightleftharpoons [(bpy^-)_2Ru(BiBzIm)Ru(EtCOO_2bpy^{2-})_2]^{4-} \quad (13)$$

Four one-electron-reduction processes at well-separated potentials are observed for asymmetrical $[(bpy)_2Ru(BiBzIm)Ru(Me_2bpy)_2]^{2+}$ (Figure 9). The first reduction potential is similar to that of $[(bpy)_2Ru(BiBzIm)Ru(bpy)_2]^{2+}$ but 100 mV less negative than that of $[(Me_2bpy)_2Ru(BiBzIm)Ru(Me_2bpy)_2]^{2+}$. Thus, the bpy ligand in the $Ru(bpy)_2$ moiety of the asymmetric

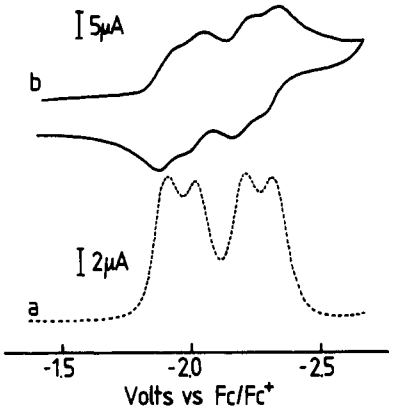

Figure 9. Differential pulse voltammogram (a) (scan rate = 4 mV s^{-1}) and a cyclic voltammogram (b) (scan rate = 100 mV s^{-1}) at a glassy-carbon electrode for the reduction of $[(bpy)_2Ru(BiBzIm)Ru(Me_2bpy)_2](ClO_4)_2$ in PrCN (0.1 mol dm^{-3} TBAP) at 20 °C.

complex is first reduced and then the Me_2bpy ligand in the $Ru(Me_2bpy)_2$ moiety. The following equations apply:

$$[(bpy)_2Ru(BiBzIm)Ru(Me_2bpy)_2]^{2+} + e^- \rightleftharpoons [(bpy)(bpy^-)Ru(BiBzIm)Ru(Me_2bpy)_2]^+ \quad (14)$$

$$[(bpy)(bpy^-)Ru(BiBzIm)Ru(Me_2bpy)_2]^+ + e^- \rightleftharpoons [(bpy)(bpy^-)Ru(BiBzIm)Ru(Me_2bpy)(Me_2bpy^-)] \quad (15)$$

$$[(bpy)(bpy^-)Ru(BiBzIm)Ru(Me_2bpy)(Me_2bpy^-)] + e^- \rightleftharpoons [(bpy^-)_2Ru(BiBzIm)Ru(Me_2bpy)(Me_2bpy^-)]^- \quad (16)$$

$$[(bpy^-)_2Ru(BiBzIm)Ru(Me_2bpy)(Me_2bpy^-)]^- + e^- \rightleftharpoons [(bpy^-)_2Ru(BiBzIm)Ru(Me_2bpy^-)_2]^{2-} \quad (17)$$

In contrast to the metal-based-oxidation processes the ligand-based-reduction processes for $[(bpy)_2Ru(BiBzIm)Os(bpy)_2]^{2+}$ show relatively similar behavior to that of the symmetrical $[(bpy)_2Ru(BiBzIm)Ru(bpy)_2]^{2+}$. This result confirms that the reduction processes are little affected by changing the metal from Ru to Os as predicted for ligand based processes.

Conclusions

The reduction processes in BiBzIm-bridged Ru or Os dinuclear complexes are ligand-based. The reduction potentials are determined by the π^* orbital energy levels of the ligands and the strength of the ligand–ligand, metal-mediated ligand–ligand, or bridging-ligand-mediated ligand–ligand interactions arising from the electron repulsion. In contrast, the oxidation potentials are metal-based, with the osmium complexes being easier to oxidize than the ruthenium analogues.

Acknowledgment. M.H. gratefully acknowledges financial support from the Ministry of Education for a Grant-in-Aid for Scientific Research, No. 63540483, and the Okasan-Kato Foundation.